

A flexible heliac configuration

This content has been downloaded from IOPscience. Please scroll down to see the full text.

1985 Nucl. Fusion 25 623

(<http://iopscience.iop.org/0029-5515/25/5/005>)

View [the table of contents for this issue](#), or go to the [journal homepage](#) for more

Download details:

IP Address: 139.184.14.159

This content was downloaded on 08/09/2015 at 02:39

Please note that [terms and conditions apply](#).

LETTERS

A FLEXIBLE HELIAC CONFIGURATION

J.H. HARRIS, J.L. CANTRELL*, T.C. HENDER,
B.A. CARRERAS, R.N. MORRIS* (Oak Ridge
National Laboratory, Oak Ridge, Tennessee,
United States of America)

ABSTRACT. The addition of an $\ell = 1$ helical winding to the heliac central conductor adds a significant degree of flexibility to the configuration by making it possible to control the rotational transform and shear. Such control is essential for an experiment because the presence of low-order resonances in the rotational transform profile can cause breakup of the equilibrium magnetic surfaces. The use of the additional winding also permits a reduction of the total central conductor current and can deepen the magnetic well.

Helical-axis stellarators with high rotational transform, low shear ($d\epsilon/dr \approx 0$) and an average magnetic well have been shown theoretically to be capable of stably confining plasmas with beta greater than 10% in the infinite-aspect-ratio limit [1–4]. A relatively simple coil set – the heliac [4] – has been proposed as a finite-aspect-ratio realization of such a configuration. However, both analytic [5] and numerical [6, 7] studies of finite-aspect-ratio, three-dimensional (3-D) equilibria have shown that the growth of finite plasma-pressure-induced field harmonics resonant at rational values of the rotational transform can lead to the formation of large magnetic islands. These islands break up the equilibrium flux surfaces at low beta values, which would presumably lead to a significant deterioration of confinement in an experiment. Similar effects have already been observed for $\beta \lesssim 1\%$ in the circular-axis, low-shear Wendelstein VIIA device [8], which has a fairly low transform per period ($\epsilon/M \sim 0.1$). Heliac configurations typically have higher values of $\epsilon/M \gtrsim 0.3$; this greatly increases the number and strength of the potential low-order resonances [5, 7, 9]. It is important, therefore, to have a means of rotational transform profile control in an experimental heliac device in order to explore (and ultimately avoid) the dangerous resonances.

* Computing and Telecommunications Division,
Martin Marietta Energy Systems, Inc.

In this letter we show that the incorporation of an $\ell = 1$ helical winding into the hardcore of the heliac configuration (Fig. 1) introduces an extra degree of freedom that can be used to control the rotational transform profile; this technique could be valuable in both the design and operation of a heliac device. The additional winding can incidentally lead to a deepening of the magnetic well. This finding is in qualitative agreement with the physical reasoning in early papers [10–12] on this general type of configuration, as well as with a more recent calculation by Yoshikawa [13], who showed that an $\ell = 2$ hardcore could be used to produce a magnetic well in a heliac configuration that otherwise would not have $V'' < 0$ everywhere.

To elucidate some of the properties of the heliac with an $\ell = 1$ hardcore winding, it is useful to consider a simple analytic model. In the helically symmetric limit, the helical flux function is given by [10–12, 14]:

$$\psi = \frac{B_0}{R_0} \frac{r^2}{2} - \frac{\mu_0 I}{2\pi} \ln r - r \left[a_1 I_1' \left(\frac{r}{R_0} \right) + b_1 K_1' \left(\frac{r}{R_0} \right) \right] \cos \left(\theta - \frac{z}{R_0} \right) \quad (1)$$

where only the dominant helical terms are retained and I_1 and K_1 are modified Bessel functions. The first term in Eq.(1) represents a uniform toroidal field of strength B_0 , while the second term results from the net longitudinal current I flowing in the central conductor and the unidirectional $\ell = 1$ hardcore winding. The I_1 and K_1 helical terms are due, respectively, to the 'external' $\ell = 1$ field (which in a heliac is generated by the helical displacement of the toroidal field coils) and the 'internal' $\ell = 1$ field of the helical hardcore.

The magnetic axis (0-point) is the turning point of Eq.(1), with $\theta = z/R_0$ and $r = r_A$, where

$$\frac{r_A}{R_0} - \frac{\mu_0 I}{2\pi R_0 B_0} \frac{R_0}{r_A} = \frac{R_0}{r_A} \left(\frac{r_A^2}{R_0^2} + 1 \right) \left[\frac{a_1}{B_0} I_1 \left(\frac{r_A}{R_0} \right) + \frac{b_1}{B_0} K_1 \left(\frac{r_A}{R_0} \right) \right] \quad (2)$$

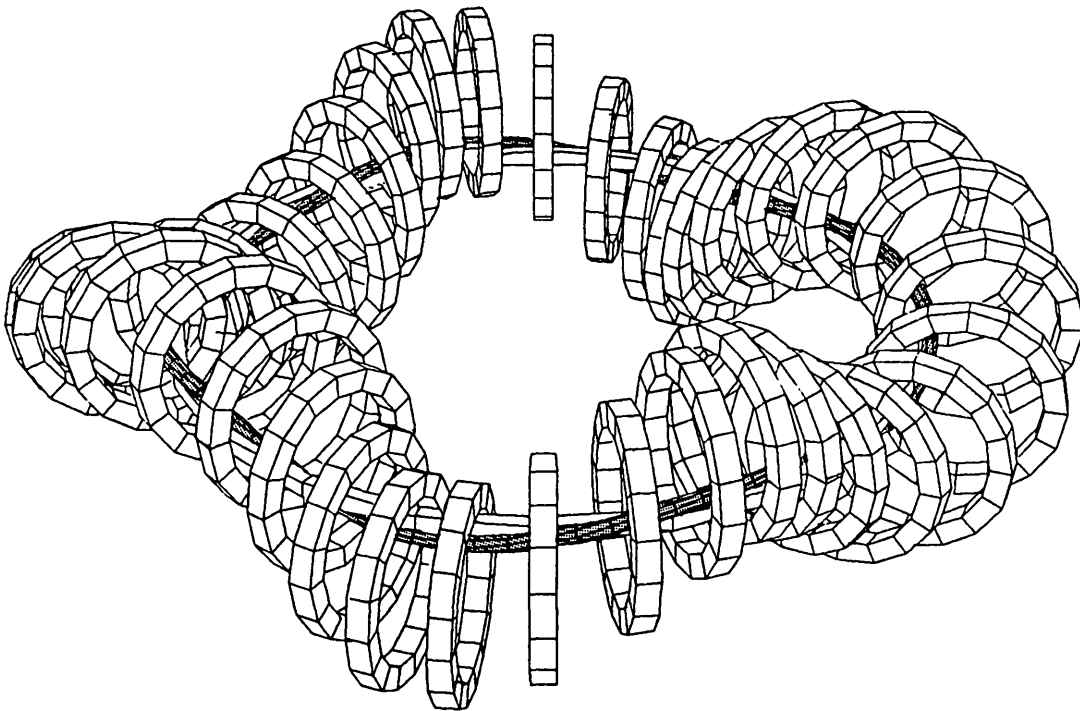


FIG.1. Coil set for modified heliac configuration, showing additional $l = 1$ hardcore winding (shaded).

Expanding in a Taylor series about the magnetic axis, we find that the ellipticity of the magnetic surfaces is

$$e = \left[\frac{\partial^2 \psi}{\partial r^2} / \left[\frac{1}{r_A^2} \frac{\partial^2 \psi}{\partial \theta^2} \left(1 + \frac{r_A^2}{R_0^2} \right) \right] \right]^{1/2} \quad (3)$$

where the second derivatives are evaluated at $r = r_A$. The $(1 + r_A^2/R_0^2)$ term in Eq.(3) occurs because we require the ellipticity to be in the plane normal to the magnetic axis. The ellipticity is directly related to the rotational transform per field period at the magnetic axis [12] by

$$\frac{\epsilon_0}{M} = 1 - \frac{2e}{e^2 + 1} \frac{1}{(1 + r_A^2/R_0^2)^{1/2}} \quad (4)$$

From Eqs (1) and (3), we find

$$\frac{\mu_0 I}{2\pi R_0 B_0} = \frac{a_1 r_A}{4B_0 R_0} \left[\left(\frac{r_A^2}{R_0^2} + e^2 - 1 \right) I_0 \left(\frac{r_A}{R_0} \right) \right.$$

$$\begin{aligned} &+ \left(e^2 + 3 + \frac{r_A^2}{R_0^2} \right) I_2 \left(\frac{r_A}{R_0} \right) \Bigg] \\ &- \frac{b_1 r_A}{4B_0 R_0} \left[\left(\frac{r_A^2}{R_0^2} + e^2 - 1 \right) K_0 \left(\frac{r_A}{R_0} \right) \right. \\ &\left. + \left(e^2 + 3 + \frac{r_A^2}{R_0^2} \right) K_2 \left(\frac{r_A}{R_0} \right) \right] \end{aligned} \quad (5)$$

Given any three of the quantities I , a_1 , b_1 , e and ϵ_0/M , the others may be determined from Eqs (3) through (5). In examining Eq.(5), it is clear that, for a given a_1 and ellipticity (or equivalently ϵ_0), as b_1 increases, the required I decreases. Physically, this means that for maintaining constant ϵ_0 we require less total current in the hardcore as the current in the helical hardcore is increased. There is a further effect that decreases the current I when b_1/B_0 increases. This is due to the change of magnetic axis position with b_1/B_0 , as can be seen from Eq.(2). Figure 2 shows the reduction of the current I with b_1/B_0 for

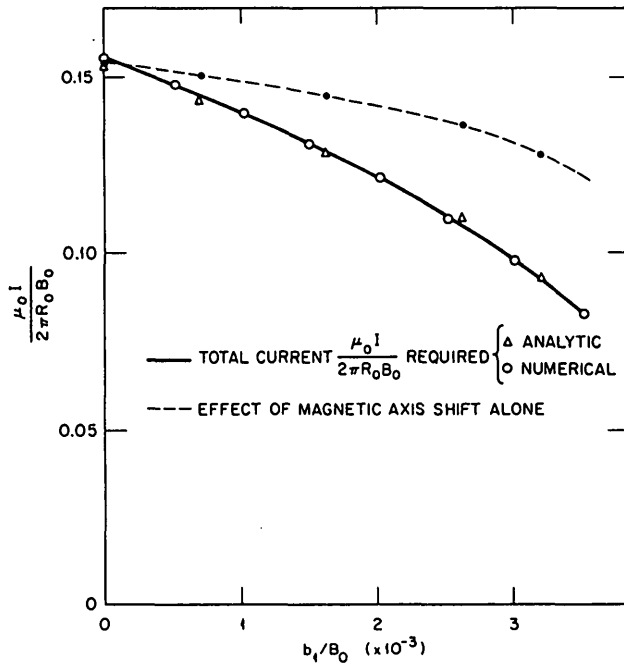


FIG.2. For a helically symmetric field model, the net longitudinal hardcore current I required to maintain constant $\epsilon_0/M = 0.3$ decreases as the $\ell = 1$ helical hardcore field component b_1 is increased. For this example, $a_1/B_0 = 0.25$ in Eq.(1).

the particular parameters $a_1/B_0 = 0.25$ and $\epsilon_0/M = 0.3$. This figure shows both the variation in hardcore current I due to increasing b_1 and the variation in I due to the magnetic axis shift (Eq.(2)) alone. Also plotted in Fig.2 are results from numerical field-line tracing calculations using the helical flux given by Eq.(1). The analytic and numerical results are in good agreement.

Using the expressions given in Ref.[12], we can also compute V'' at the magnetic axis:

$$V'' = \frac{2}{R_0 B_0^2 e^2 (1 + r_A^2/R_0^2)^{3/2}} \times \left[\frac{r_A^2}{R_0^2} - \frac{e^2 - 1 - r_A^2/R_0^2}{1 + r_A^2/R_0^2} \left(\frac{R_0}{2r_A} \frac{a_1 I_1 + b_1 K_1}{a_1 I_1' + b_1 K_1'} - \frac{1 + r_A^2/R_0^2}{e^2 + 1 + r_A^2/R_0^2} \right) \right] \quad (6)$$

For the same parameters as in Fig.2, this expression gives $R_0 B_0^2 V'' = -0.197$ when $b_1/B_0 = 0$, and

$R_0 B_0^2 V'' = -0.497$ when $b_1/B_0 = 3.2 \times 10^{-3}$. Thus, for a fixed ϵ_0 the magnetic well gets deeper as the current in the helical hardcore is raised. Numerical field-tracing calculations also show the same result.

We have found that while helically symmetric calculations are useful as a general guide to the behaviour of the central transform and magnetic well, full 3-D calculations using a filamentary representation of the heliac coil set are necessary to accurately determine flux surface shapes and profiles of transform and V'' . This is because the existence and shape of magnetic surfaces are strongly affected by (1) the finite extent of the toroidal coils and (2) toroidal effects (which actually determine the last closed surface by introducing resonances [15]). In the calculations that follow, we represent a heliac configuration as an array of N circular coils of radius a_c , whose centres are located on a toroidal helix having major radius R_0 , minor radius r_{sw} , and M periods. For all of the calculations shown here, $N/M = 9$ coils per period. The nominal toroidal field strength is given (in amperes per metre) by $H_0 = NI_{TF}/2\pi R_0$, where I_{TF} is the toroidal field coil current. The circular centre conductor at the minor axis carries a current I_R . The helical hardcore winding carries a current I_{H1} and follows the same winding law ($\theta = M\phi$) as the toroidal field coils, but with a minor radius $a_{hc} (< a_c)$. The total (toroidally directed) current in the hardcore is $I_T = I_R + I_{H1}$. A small external vertical field of about 5% of H_0 is required to define the magnetic axis, which we usually shift toroidally outward (relative to the 'helically centred' position) by a small amount ($\Delta R/R_0 \sim 1\%$) in order to improve the magnetic well and flux surface size.

Figure 3 shows the results of 3-D field-line calculations for two heliac configurations – one with a helical hardcore winding and one without. The two configurations are essentially identical in rotational transform profile and average last closed-surface radius, but the configuration with the helical hardcore winding requires somewhat less than one-half the total toroidal hardcore current (i.e. one-half the value of $I_T/(R_0 H_0)$). This is in good agreement with the analytic calculations done in the helically symmetric limit. The profiles of V' from the field-line calculations show that the configuration with the helical hardcore has a deeper magnetic well, as is also indicated by the greater indentation in the magnetic surface shape. The increase in magnetic well is in agreement with the analytic calculations. Figure 4 shows how the axis position varies as a function of helical hardcore current for the same configuration as in Fig.3. This also shows

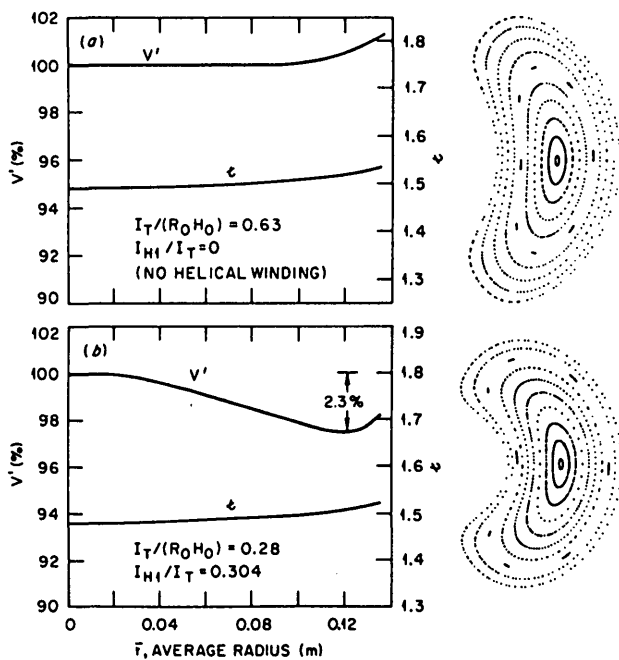


FIG.3. Comparison of ϵ and V' profiles for $M = 4$, $R/a_c = 4$ heliacs, with and without $\ell = 1$ hardcore winding. For this example, $R_0 = 1$ m, $r_{SW}/a_c = 0.7$, $a_c/a_{hc} = 6$, $\Delta R/R_0 = 0.0125$.

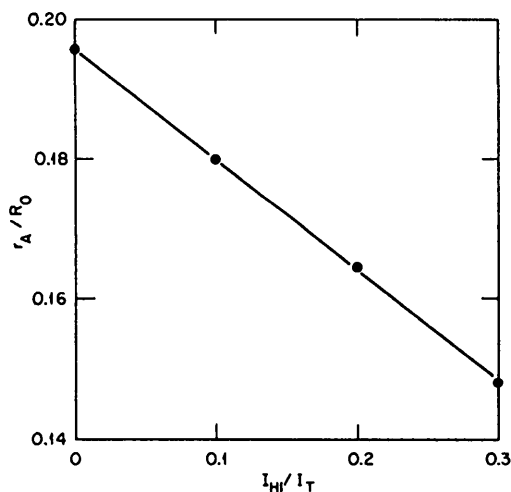


FIG.4. Magnetic axis position r_A as a function of helical hardcore current I_{H1}/I_T (other parameters as in Fig.3).

good agreement with the analytic calculations: the axis shifts helically inward (towards the hardcore) as the fraction of the current flowing in the helical winding increases.

Variation of the helical hardcore current can also provide a means to vary the shape of the rotational

transform profile. Figure 5 shows an example in which the sign of $d\epsilon/dr$ is changed by varying the fraction of the (fixed) total hardcore current flowing in the helical winding (a heliac without a helical hardcore has $d\epsilon/dr > 0$). Figure 6 shows similar plots for a configuration having the same pitch but three times the aspect ratio and number of field periods. The profiles of ϵ/M are similar to those in Fig.5, which indicates that the profile shape is determined directly by helical, rather than toroidal, effects.

A range of possible transform profiles that can be synthesized for a particular configuration is shown in Figs 7 and 8. In Fig.7 the fraction of total hardcore current carried by the helical winding is held fixed and the net hardcore current is varied, while in Fig.8 the net hardcore current is held fixed and the fraction carried by the helical winding is varied. The radius of the last closed flux surface is strongly affected by the proximity of strong resonances (e.g. $\epsilon/M = 1/2$) that break up the outer flux surfaces, as can be seen in the rotational transform profiles.

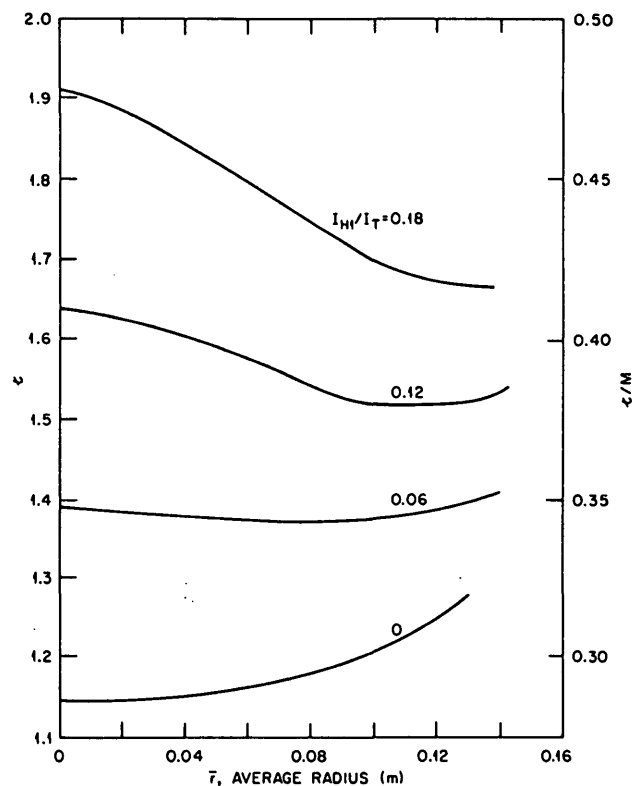


FIG.5. Effect of increasing the helical hardcore current on the ϵ profile of an $M = 4$, $R/a_c = 4$ heliac. For these calculations, $R_0 = 1$ m, $r_{SW}/a_c = 0.7$, $a_c/a_{hc} = 3.33$, $I_T/(R_0 H_0) = 0.33$.

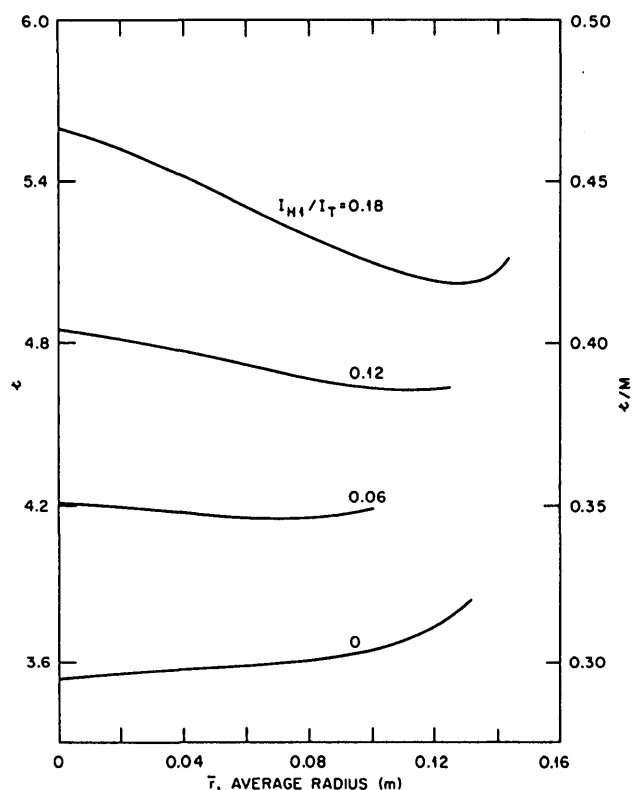


FIG. 6. Effect of increasing the helical hardcore current on the ϵ profile of a heliac, with $M = 12$, $R/a_c = 12$, and other parameters as in Fig. 3.

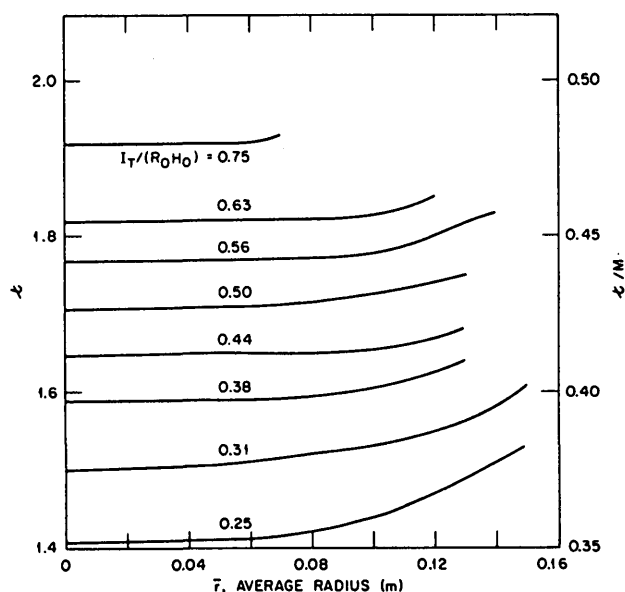


FIG. 7. Rotational transform profiles for a range of net hardcore currents in an $M = 4$, $R/a_c = 4$ heliac with a fixed helical hardcore current fraction. $I_{H1}/I_T = 0.304$ (other parameters as in Fig. 3).

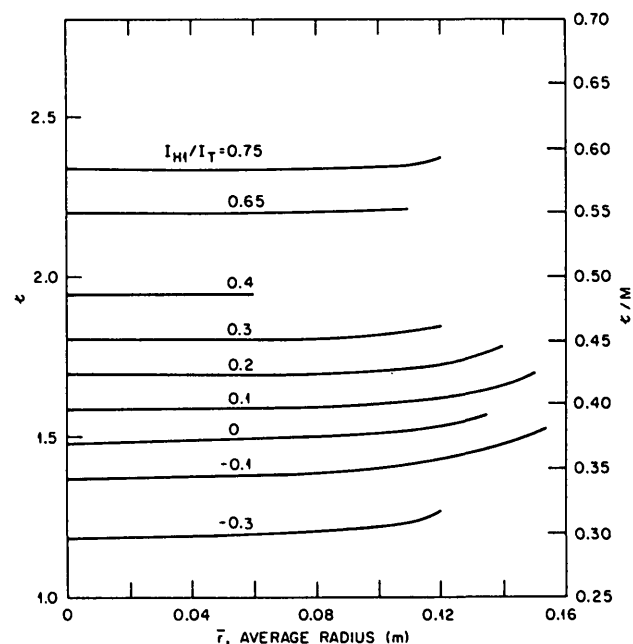


FIG. 8. Rotational transform profiles for a range of helical hardcore current fractions for the configuration of Fig. 7 with fixed net hardcore current $I_T/(R_0 H_0) = 0.63$.

Figure 9 shows flux surfaces at two positions within a field period for three configurations from the parameter scans shown in Figs 7 and 8. The plots illustrate the shapes of the magnetic surfaces obtained for widely varying ϵ/M values. For the case with the rather high value of $\epsilon_0/M = 0.552$, the magnetic axis has a large helical excursion, and toroidal effects make the surfaces rather asymmetric. This is because the coil parameters of the configuration used for the parameter scan were chosen to give optimum results in the range $\epsilon/M \lesssim 0.4$. If, for example, the helical excursion of the toroidal field coils (r_{SW}) is reduced to $r_{SW}/a_c \sim 0.5$, the optimum range of ϵ_0/M shifts upward and highly symmetric surfaces can be obtained with $\epsilon_0/M > 0.5$.

We conclude by noting that the range of rotational transform values that can be achieved in an actual device will depend on a careful design of the coil configuration, allowing sufficient space for the required windings at realistic current densities. We have carried out preliminary studies of this question which indicate that variations in ϵ/M of at least a factor of two can be readily achieved. Given the large number of design parameters involved, computer optimization techniques [16, 17] and concepts for

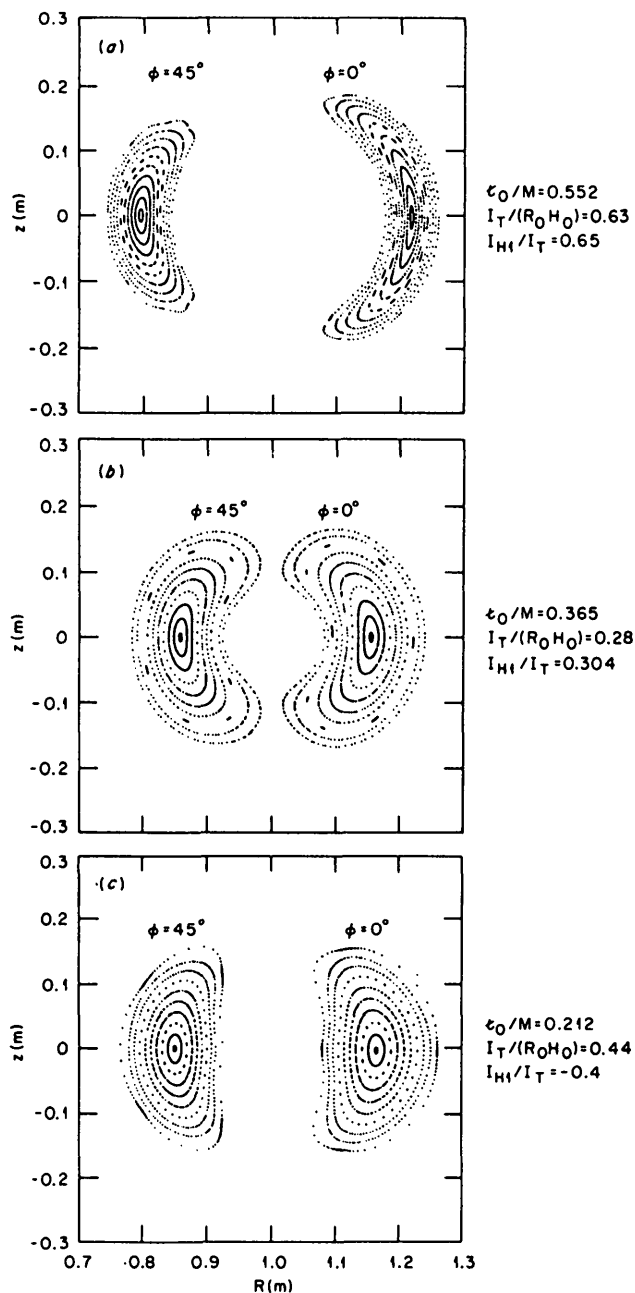


FIG.9. Flux surfaces at two positions within a field period for heliac configurations of different t_0/M values from the parameter scans shown in Figs 7 and 8.

modular heliac coils [18, 19] could be profitably applied to further improve modified heliac configurations of the type considered here.

ACKNOWLEDGEMENTS

The authors are grateful to J.A. Rome, V.E. Lynch and J. Guasp for their help in carrying out the

computations, and to J.F. Lyon for continuing support and encouragement. In addition, one of the authors (J.H.H.) acknowledges a discussion of the results of Ref.[13] with S. Yoshikawa.

This work was supported by the Office of Fusion Energy, U.S. Department of Energy, under Contract No. DE-AC05-84OR21400 with Martin Marietta Energy Systems, Inc.

REFERENCES

- [1] MONTICELLO, D.A., DEWAR, R.L., FURTH, H.P., REIMAN, A., *Phys. Fluids* **27** (1984) 1248.
- [2] MERKEL, P., NÜHRENBURG, J., GRUBER, R., TROYON, F., *Nucl. Fusion* **23** (1983) 1061.
- [3] BAUER, F., BETANCOURT, O., GARABEDIAN, P., *Magnetohydrodynamic Equilibrium and Stability of Stellarators*, Springer-Verlag, New York (1984).
- [4] BOOZER, A.H., CHU, T.K., DEWAR, R.L., FURTH, H.P., GOREE, J.A., JOHNSON, J.L., KULSRUD, R.M., MONTICELLO, D.A., KUO-PETRAVIC, G., SHEFFIELD, G.V., YOSHIKAWA, S., BETANCOURT, O., in *Plasma Physics and Controlled Nuclear Fusion Research 1982* (Proc. 9th Int. Conf. Baltimore, 1982), Vol.3, IAEA, Vienna (1983) 129.
- [5] REIMAN, A., BOOZER, A.H., *Phys. Fluids* **27** (1984) 2446.
- [6] LYON, J.F., CARRERAS, B.A., HARRIS, J.H., ROME, J.A., CHARLTON, L.A., et al., in *Plasma Physics and Controlled Nuclear Fusion Research 1982* (Proc. 9th Int. Conf. Baltimore, 1982), Vol.3, IAEA, Vienna (1983) 115.
- [7] CARRERAS, B.A., CANTRELL, J.L., CHARLTON, L.A., GARCIA, L., HARRIS, J.H., HENDER, T.C., HICKS, H.R., HOLMES, J.A., ROME, J.A., LYNCH, V.E., in *Plasma Physics and Controlled Nuclear Fusion Research 1984* (Proc. 10th Int. Conf. London, 1984), Vol.2, IAEA, Vienna (1985) 31.
- [8] WENDELSTEIN VII-A TEAM et al., *Plasma Phys. Controlled Fusion* **26** (1984) 183.
- [9] DANILKIN, I.S., SHPIGEL, I.S., *Tr. Fiz. Inst., Akad. Nauk SSSR* **65** (1973) 50.
- [10] FURTH, H.P., KILLEEN, J., ROSENBLUTH, M.N., COPPI, B., in *Plasma Physics and Controlled Nuclear Fusion Research* (Proc. Conf. Culham, 1965), Vol.1, IAEA, Vienna (1966) 103.
- [11] McNAMARA, B., WHITEMAN, K.J., TAYLOR, J.B., *ibid.*, p.145.
- [12] ZUEVA, N.M., SOLOV'EV, L.S., *Plasma Phys.* **8** (1966) 765.
- [13] YOSHIKAWA, S., *Nucl. Fusion* **23** (1983) 667.
- [14] PORITSKY, H., *J. Appl. Phys.* **30** (1959) 1828.
- [15] CARY, J., *Phys. Fluids* **27** (1984) 119.
- [16] CHODURA, R., DOMMASCHK, W., HERRNEGGER, F., LOTZ, W., NÜHRENBURG, J., SCHLÜTER, A., *IEEE Trans. Plasma Sci.* **9** (1981) 221.

- [17] BUTCHER-EHRHARDT, A., in Fifth International Workshop on Stellarators (Proc. IAEA Tech. Committee Meeting on Plasma Confinement and Heating in Stellarators, Schloss Ringberg), Commission of the European Communities, Directorate-General XII – Fusion Programme, Brussels, EUR-9618-EN (1984) 717.
- [18] REIMAN, A., BOOZER, A.H., Phys. Fluids **26** (1983) 496.
- [19] HARMEYER, E., KISSLINGER, J., RAU, F., WOBIG, H., in Plasma Physics and Controlled Nuclear Fusion Research 1984 (Proc. 10th Int. Conf. London, 1984), Vol.3, IAEA, Vienna (1985) H-II-4.

(Manuscript received 17 January 1985)

TOROIDAL EQUILIBRIUM WITH LOW-FREQUENCY WAVE-DRIVEN CURRENTS

D.A. EHST (Fusion Power Program, Argonne National Laboratory, Argonne, Illinois, United States of America)

ABSTRACT. In the absence of an emf, the parallel current, j_{\parallel} , in a steady-state tokamak will consist of a neoclassical portion plus a wave-driven contribution. Using the drift kinetic equation, the quasi-linear (wave driven) current is computed for high-phase-speed waves in a torus, and this is combined with the neoclassical term to obtain the general expression for the flux surface average $\langle j_{\parallel} \rangle$. For a given pressure profile this technique fully determines the MHD equilibrium, permitting the study of a new class of toroidal equilibria.

In calculations of tokamak MHD equilibrium, two functions of ψ , the poloidal flux, must be specified at the outset. In one conventional approach [1], for example, the pressure, p , and the diamagnetism, $F = RB_t$, are input to the problem, and the current density, j , and the safety factor, q , are determined by solving the Grad-Shafranov equation. Inasmuch as the input functions are frequently taken to be independent of each other, an unlimited variety of equilibria results. Thus, by choosing different models for $F(\psi)$, various current profiles $j(r)$ can satisfy equilibrium for a given $p(\psi)$. This degree of arbitrariness can, however, be removed if j can be related to p . For inductively driven tokamaks, this might be accomplished with the aid of Ohm's law. Alternatively, as we will show, the equilibrium is fully determined if it is sustained by steady-state RF (wave) current drive. In this case the current density consists of two distinct terms, $j = j^{NC} + j^{QL}$. The neoclassical current, j^{NC} , arises from the magnetic drifts of charged particles in

the inhomogeneous magnetic field and is a known function of the plasma density and temperature profiles [2]. The quasi-linear current, j^{QL} , due to velocity space diffusion with an RF current driver, can also be calculated from a knowledge of the density and temperature profiles if the spatial deposition of the driver power is computed [3]. Consequently, for given density and temperature [and, hence, $p(\psi)$] profiles a unique j exists with steady-state RF current drive, and it is possible to infer the actual $F(\psi)$ which is needed to solve for MHD equilibrium. The goal of this brief letter is the derivation of that equation which determines $F(\psi)$; actual numerical computation of two-dimensional RF-sustained equilibria will be deferred to future reports.

We consider an axisymmetric tokamak plasma with orthogonal co-ordinates ψ , χ , and ξ . The magnetic field and the poloidal flux are given by $\vec{B} = F \nabla \xi + \nabla \psi \times \nabla \psi / 2\pi$, where $\nabla \psi = \hat{\psi} 2\pi R B_p$ and $\nabla \xi = \hat{\xi} / R$. ($\hat{\cdot}$ indicates a unit vector.) R is the distance from the symmetry axis, and B_t and B_p are, respectively, the toroidal (ξ) and poloidal (χ) field components.

It is easily shown [1] that the equilibrium pressure and diamagnetism are functions of only the poloidal flux, and that ψ satisfies the Grad-Shafranov equation:

$$-4\pi^2 \left(\mu_0 R^2 \frac{dp}{d\psi} + F \frac{dF}{d\psi} \right) = R^2 \nabla \cdot \left(\frac{\nabla \psi}{R^2} \right) \quad (1)$$

The object of our study is to find the function $F(\psi)$ which is generated by non-inductively driven tokamak currents, which, with the aid of Eq.(1), can be used to fully determine the two-dimensional equilibrium.

We begin by noting that in equilibrium the current density parallel to the magnetic field is given by

$$j_{\parallel} = \frac{-2\pi F}{B} \frac{dp}{d\psi} - \frac{2\pi B}{\mu_0} \frac{dF}{d\psi} \quad (2)$$